Supplementary Information

Climate change and deforestation drive the displacement and contraction of tropical montane cloud forests

Santiago Ramírez-Barahona, Angela P. Cuervo-Robayo, Kenneth Feeley, Andrés Ortiz-Rodríguez, Antonio A Vásquez-Aguilar, Juan Francisco Ornelas, Hernando Rodríguez-Correa

This file contains

- Supplementary tables S1–S3
- Supplementary figures S1–S9.
- Data and code available at *Zenodo* with the identifier: doi.org/10.5281/zenodo.5587220

Supplementary tables

Supplementary table S1. Historical altitudinal trends for vascular plant species across Mesoamerican cloud forests over the period 1901–2016. Model coefficients estimated for the species' upper range limits using a Piecewise Growth Model with two time periods: 1901–1975 (pre-breakpoint) and 1976–2016 (post-breakpoint).

group	term	estimate	std.error
	Intercept	1,632.31	36.91
	pre-breakpoint slope	19.31	1.95
	post-breakpoint slope	-41.38	4.12
Species	Intercept	725.51	
Species	pre-breakpoint slope	33.15	
Species	post-breakpoint slope	75.99	
	Residual	201.83	

Supplementary table S2. Historical altitudinal trends for vascular plant species across Mesoamerican cloud forests over the period 1901–2016. Model coefficients estimated for the species' range mid-points using a Piecewise Growth Model with two time periods: 1901–1975 (pre-breakpoint) and 1976–2016 (post-breakpoint).

group	term	estimate	std.error
	Intercept	1,058.80	33.13
	pre-breakpoint slope	2.89	1.66
	post-breakpoint slope	-7.82	3.18
Species	Intercept	660.73	
Species	pre-breakpoint slope	29.52	
Species	post-breakpoint slope	59.39	
	Residual	147.73	

Supplementary table S3. Historical altitudinal trends for vascular plant species across Mesoamerican cloud forests over the period 1901–2016. Model coefficients estimated for the species' lower range limits using a Piecewise Growth Model with two time periods: 1901–1975 (pre-breakpoint) and 1976–2016 (post-breakpoint).

group	term	estimate	std.error
	Intercept	600.39	24.42
	pre-breakpoint slope	-10.08	1.42
	post-breakpoint slope	14.94	3.08
Species	Intercept	473.69	
Species	pre-breakpoint slope	24.034	
Species	post-breakpoint slope	56.87	
	Residual	150.42	

Supplementary figures

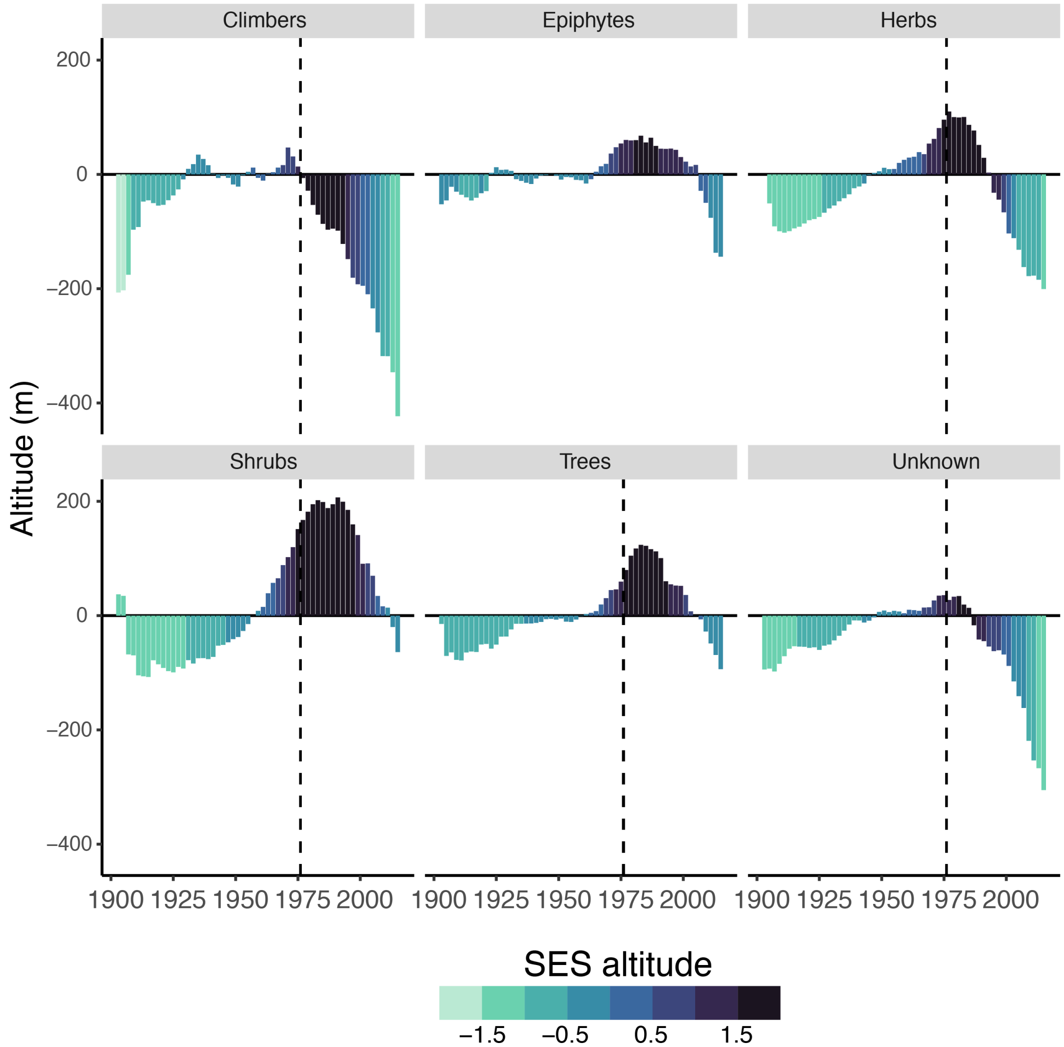

Supplementary figure S1. Historical mean altitudinal trends for the upper range limits across Mesoamerican cloud forest plant species over the period 1901–2016. a–c, bi-yearly mean deviations from baseline averages (that is, species' average during 1901–1975) for the upper limit of species' ranges. Species estimates are grouped by growth form. Estimates are based on the first derivative of the fitted smoothing splines averaged across individual species. Colour scale represents the mean Standardized Effect sizes (SES) across species estimated through simulations. Estimates are based on the predicted values of the fitted smoothing splines. Vertical dashed lines in a–d indicate the pre-defined breakpoint (that is, 1975–1976).

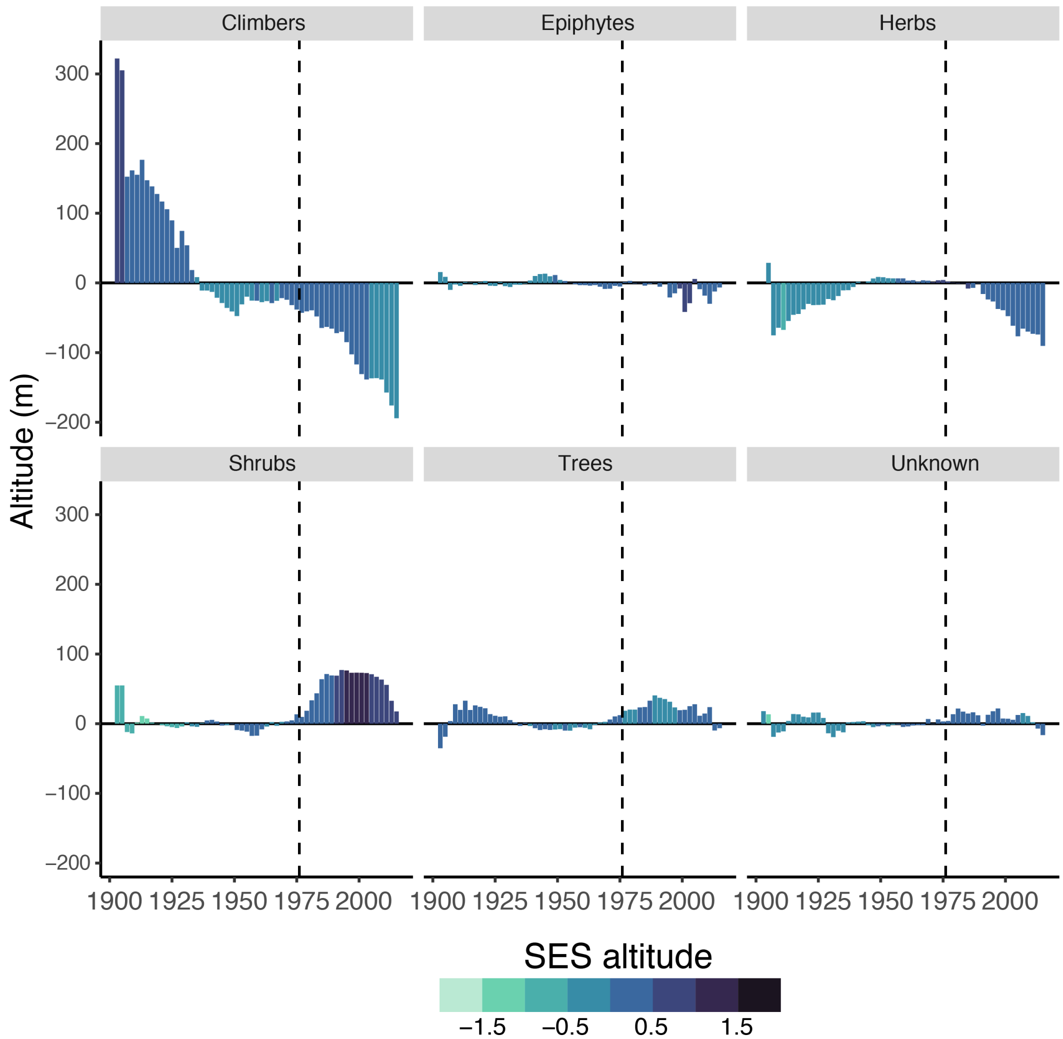

Supplementary figure S2. Historical mean altitudinal trends for the mid-range point across Mesoamerican cloud forest plant species over the period 1901–2016. a–c, bi-yearly mean deviations from baseline averages (that is, species' average during 1901–1975) for the upper limit of species' ranges. Species estimates are grouped by growth form. Estimates are based on the first derivative of the fitted smoothing splines averaged across individual species. Colour scale represents the mean Standardized Effect sizes (SES) across species estimated through simulations. Estimates are based on the predicted values of the fitted smoothing splines. Vertical dashed lines in a–d indicate the pre-defined breakpoint (that is, 1975–1976).

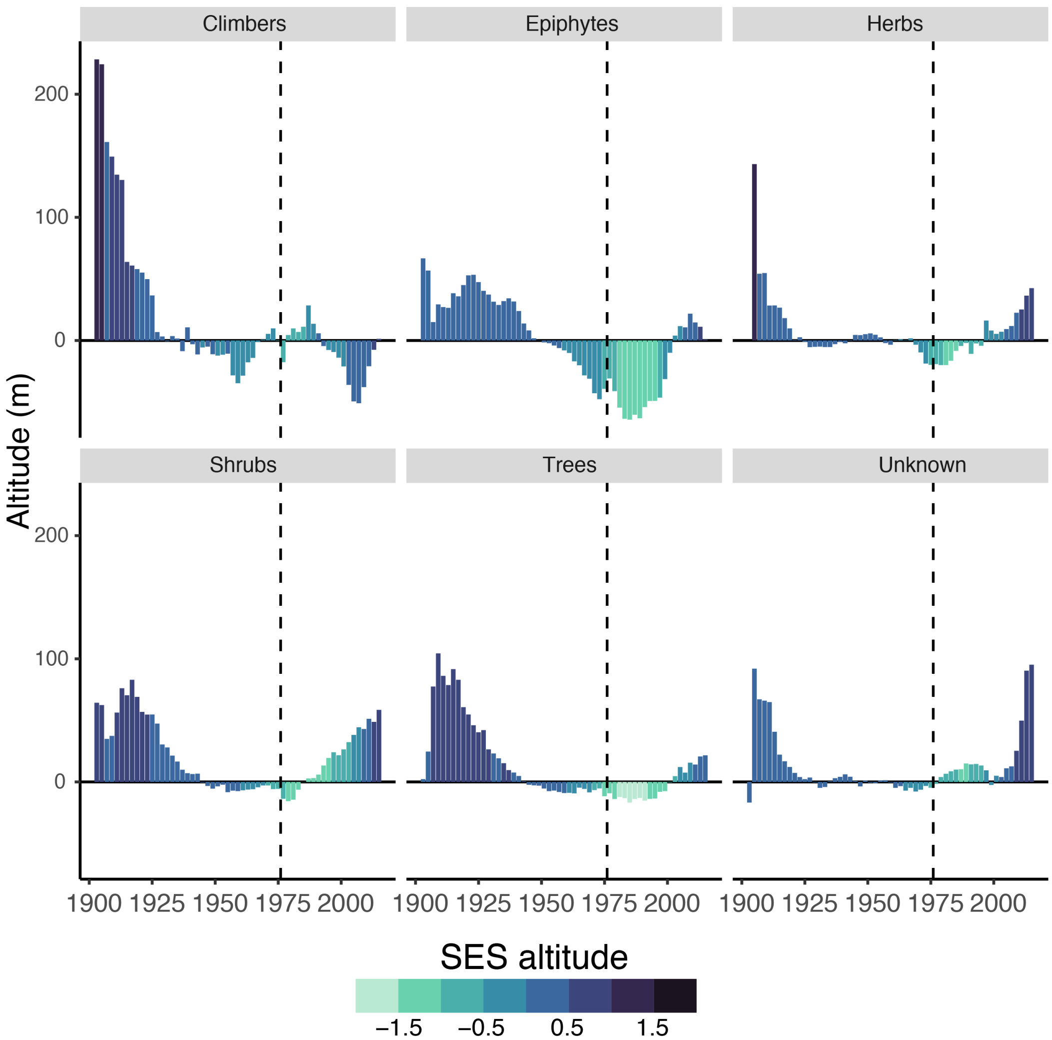

Supplementary figure S3. Historical mean altitudinal trends for the lower range limits across Mesoamerican cloud forest plant species over the period 1901–2016. a–c, bi-yearly mean deviations from baseline averages (that is, species' average during 1901–1975) for the upper limit of species' ranges. Species estimates are grouped by growth form. Estimates are based on the first derivative of the fitted smoothing splines averaged across individual species. Colour scale represents the mean Standardized Effect sizes (SES) across species estimated through simulations. Estimates are based on the predicted values of the fitted smoothing splines. Vertical dashed lines in a–d indicate the pre-defined breakpoint (that is, 1975–1976).

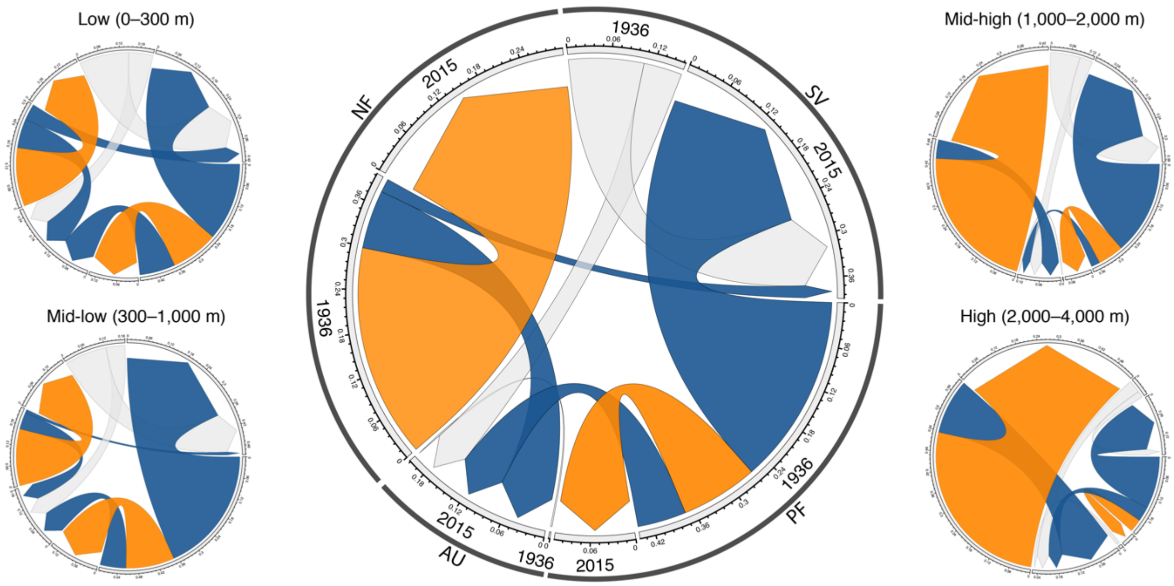

Supplementary figure S4. Transitions in land-use categories across Mesoamerican cloud forests localities over the period 1936–2015. Chord diagram showing the proportional ‘flow’ among the four land-use categories btween two years (1936 and 2015): Agriculture-urban (AU), Primary forests (PF), Non-forest vegetation (NF), and Secondary vegetation (VG). The centrtal larger circle represents land-use transitions across all grid-cells and smaller circles represen land-use transitions estimated across four altitudinal belts: Low (0-300 m), Middle-low (300–1,000 m), Middle-high (1,000–2,000), and High (>2,000 m). In all cases, flows for the PF and NF categories are highlighted to represent permanence within the same primary vegetation category (orange or light grey) or transition into other categories (blue or dark grey). The width of the flows represents the proportion of grid-cells transitioning among categories/years. The size of the fragments in the outer circles is proportional to the number of grid-cells within each category per year, where the sum of the four categories for each year equals one.

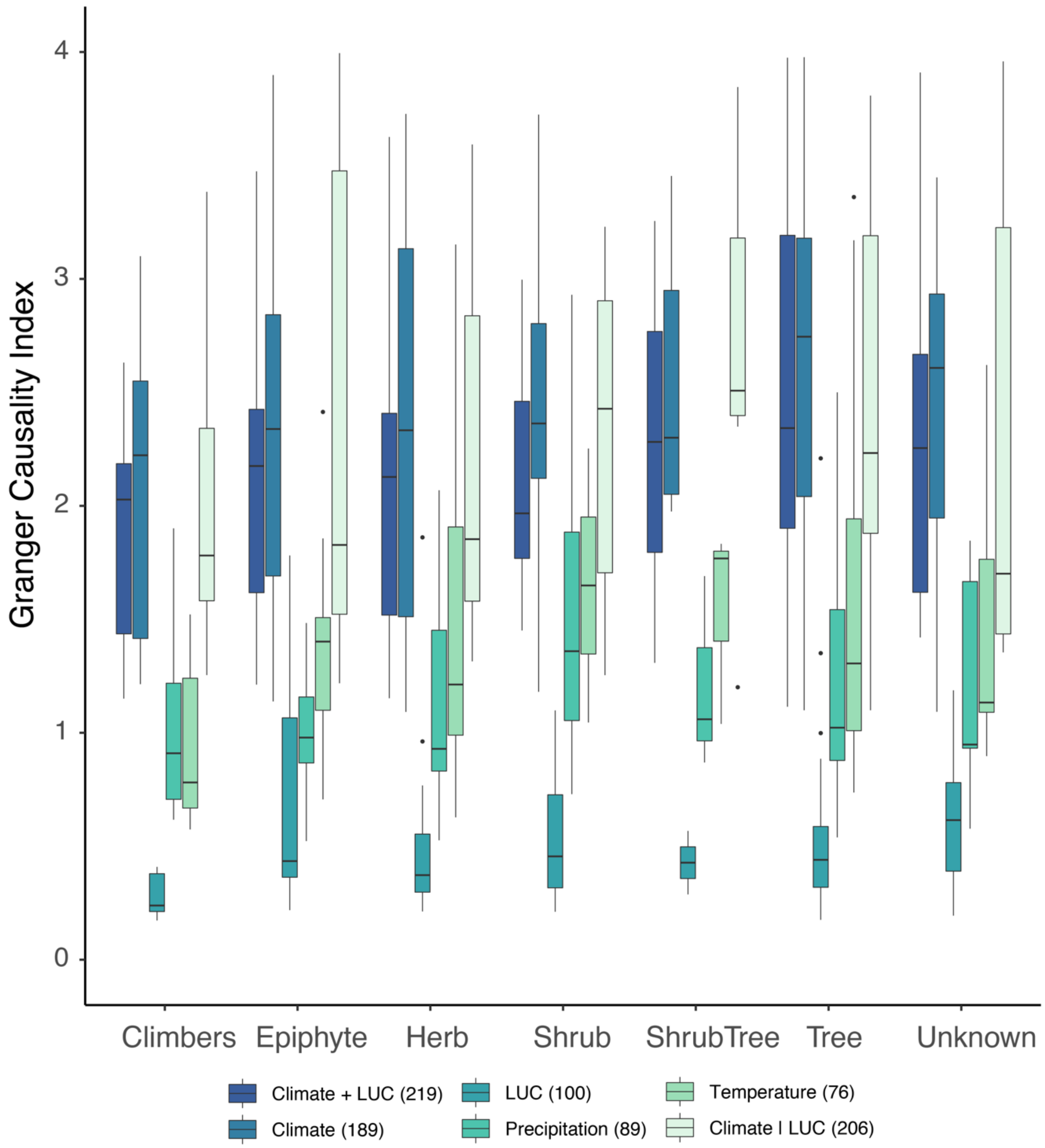

Supplementary figure S5. Granger causal influence of climate and land-use change time series on species historical trends of species upper range limits over the period 1901–2016. Boxplots showing the distribution of the per-species Granger Causality Index (GCI) of the different climate change land-use time series. Species estimates are grouped by growth form. All estimates are for species with a significant GCI (p-value $<$ 0.05).

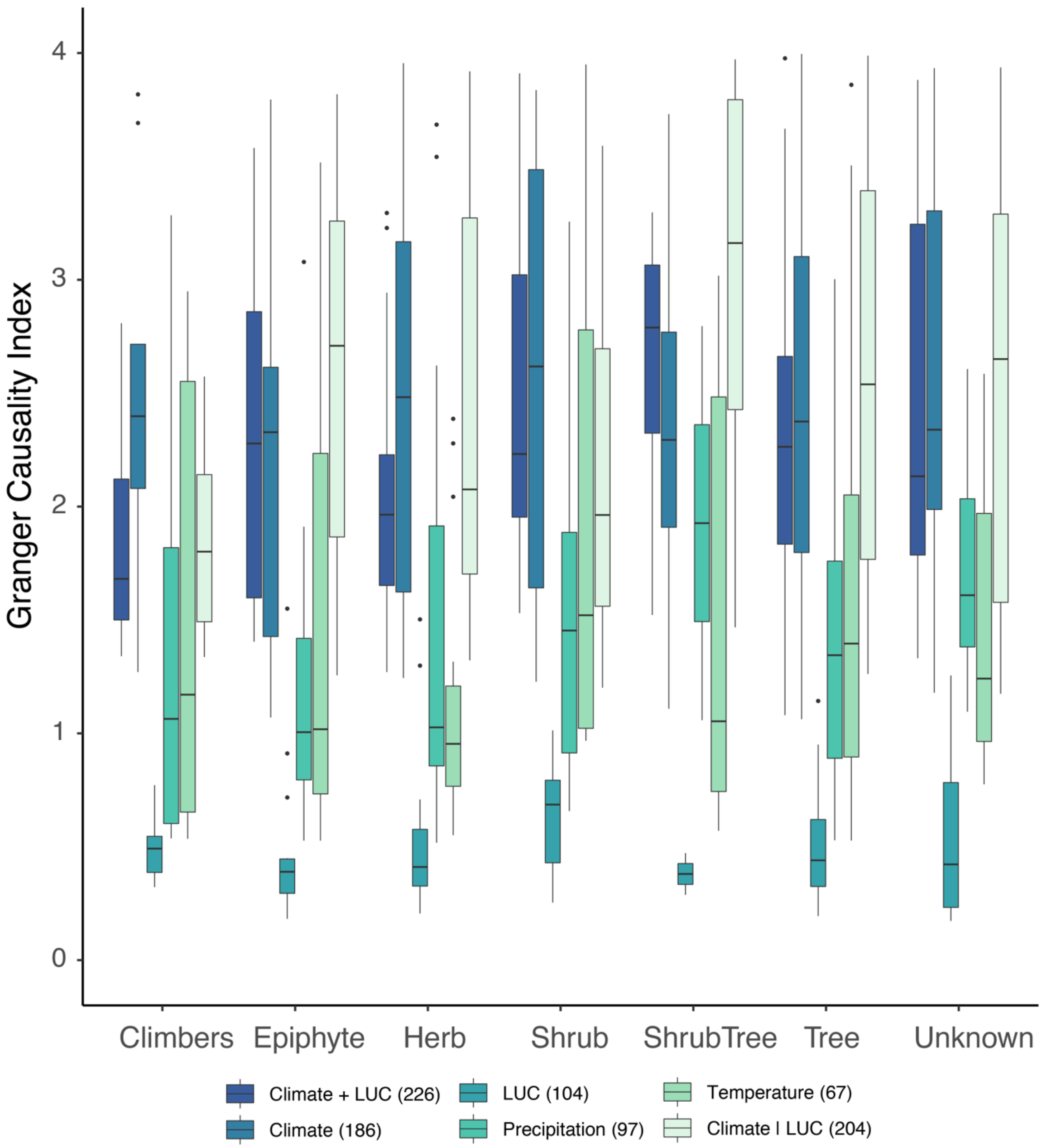

Supplementary figure S6. Granger causal influence of climate and land-use change time series on species historical trends of species mid-range point over the period 1901–2016. Boxplots showing the distribution of the per-species Granger Causality Index (GCI) of the different climate change land-use time series. Species estimates are grouped by growth form. All estimates are for species with a significant GCI (p-value < 0.05).

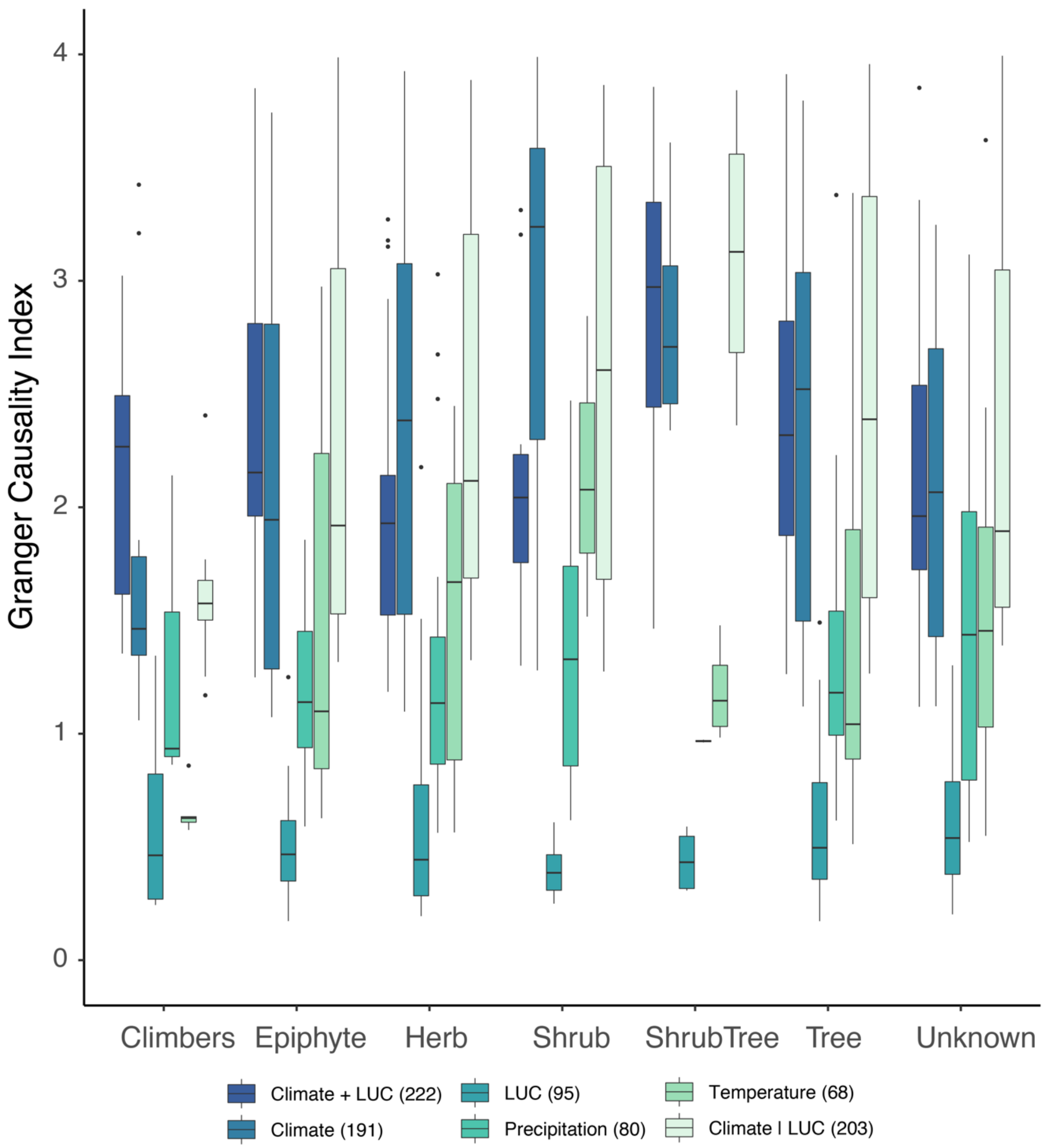

Supplementary figure S7. Granger causal influence of climate and land-use change time series on species historical trends of species lower range limits over the period 1901–2016. Boxplots showing the distribution of the per-species Granger Causality Index (GCI) of the different climate change land-use time series. Species estimates are grouped by growth form. All estimates are for species with a significant GCI (p-value < 0.05).